

CALIBRATION AND VALIDATION OF PLASTIC HIGH STRAIN RATE MODELS FOR ALLOY 718

Ted Sjöberg^{*1}, K. G. Sundin¹, Mats Oldenburg¹

¹Division of Solid Mechanics, Luleå University of Technology, SE-97187 Luleå, Sweden

* E-mail: ted.sjoberg@ltu.se

Keywords: Alloy 718, Johnson-Cook, Zerilli-Armstrong, Experimental analysis, Parameters

Summary: Alloy 718 (Inconel™ 718), composed mainly of nickel, iron and chromium has properties that are of interest in many high temperature applications. One such application is the containment structure in aero engines which prevents fragments from penetrating the structure in case of blade failure. Impact of blade fragments on the containment structure includes both high strain rates and high temperatures and simulation models must therefore have their base in experimental conditions including transient loading and heating. An experimental method has been developed that utilizes induction heating in a high rate tensile test machine. Strain rates up to the order of 1000 s^{-1} and temperatures up to 650 °C have been included in the test program. Material parameters for the Johnson-Cook and the Zerilli-Armstrong models are evaluated from experimental data using optimisation. These parameters are then used to simulate a specially designed impact experiment and a direct comparison of a calculated and measured quantity can be made in order to validate model and parameters. The result from the validation experiment showed better agreement for the Johnson-Cook model than the Zerilli-Armstrong model.

1 INTRODUCTION

Material testing will continue to be a very important activity in mechanical laboratories until physically based models have reached sufficient quality so that mechanical properties can be predicted from microstructural features. Until then the development of experimental techniques for mechanical testing will continue and more and better data for calibration of the empirically based models that still dominate simulation of plastic processes will be provided. Advanced modern methods for material characterisation are often based on digital photographic information from deforming specimens. Development of the strain field during loading is studied and there are several methods to determine a material's constitutive equations from such information [1].

The traditional method for material characterisation is to use a conventional straight tensile specimen which has a homogeneous state of stress and strain. This method is straightforward

and in its simplest form it gives useful data regarding plasticity up to the point where necking of the specimen sets in. In this paper the traditional method with straight specimens loaded in tension has been extended to high strain rates and high temperatures which introduce difficulties regarding measurement techniques. Testing at combinations of high strain rates and high temperatures is commonly performed in Split Hopkinson Bar arrangements with a heating device (see e.g. [2]) but here a high-speed hydraulic machine was used for which inductive heating was developed. A non-contacting method for measurement of elongation was adapted to the situation.

The investigated material is the so called Alloy 718 which is used in for example the hot section of aero engines because of its favourable high-temperature properties. For simulation of impact events on the containment structure at operating conditions, caused for example by blade fracture, a good model for plastic behaviour at combined high temperature and high strain-rate is needed. A few suggestions for such simulation models have been found in literature [3-6], but methods for parameter estimation are not always well described and validation is generally lacking. This paper presents experimental methods for calibration of material models, the extraction of model parameters and an impact experiment for the validation of models and parameters.

2 PROBLEM AND METHOD

2.1 Presentation of the problem

Two common models for plasticity in metals that include high strain-rates as well as high temperatures are the Johnson-Cook (JC) [7] and the Zerilli-Armstrong (ZA) [8] models. The JC-model is fully empirical and the ZA-model is based on simplified dislocation mechanics. This work is limited to the study of these two models. The JC model is written

$$\sigma_y = (A + B\varepsilon_p^n) \left(1 + C \ln \left(\frac{\dot{\varepsilon}_p}{\dot{\varepsilon}_{0p}} \right) \right) (1 - T^{*m}) \quad (1)$$

where σ_y is the Mises yield stress, ε_p is the equivalent plastic strain, $\dot{\varepsilon}_p$ and $\dot{\varepsilon}_{0p}$ are the current and reference strain rate respectively and $T^* = (T - T_r)/(T_m - T_r)$ is the homologous temperature. Here T is the current temperature and T_r and T_m is a reference temperature and the melting temperature respectively. A , B , C , n and m are model parameters. The general form of the ZA-model is written

$$\sigma_y = \sigma_a + A\varepsilon_p^{1/2} e^{-(\alpha_0 - \alpha_1 \ln(\dot{\varepsilon}_p))T} + B e^{-(\beta_0 - \beta_1 \ln(\dot{\varepsilon}_p))T} \quad (2)$$

where T is the absolute temperature and the constants σ_a , A , α_0 , α_1 , B , β_0 , and β_1 are material parameters. In eq (2) a term that is influenced by the grain size is incorporated in the parameter σ_a . The number of model parameters in eq (1) and (2) are 5 and 7 respectively. In order to use the models in a practical simulation the parameters must be determined.

The final choice of which model to use is based on a comparison of predictive power in a relevant situation. Therefore the process of establishing a simulation model can be said to follow three steps: (i) A set of well controlled calibration experiments must be designed and

performed in which important physical factors cover the interval which is expected in the application. (ii) From the output data of these experiments parameters in the model must be extracted using established and reliable methods. (iii) A validation experiment with relevant physical conditions must be designed and performed which can be simulated using the model and parameters and which makes direct comparison possible between experimental and simulated quantities.

In this work the material of interest is Alloy 718 (or Inconel™ 718) which has been aged by GKN Aerospace Sweden AB in an approach comparable to the instructions from the manufacturers (Haynes International LTD). The material is in the form of 1.6 mm thick sheets and abrasive water cutting is used to cut out the specimens.

2.2 Calibration experiments

First a conventional tensile test series with specimens taken 0°, 45° and 90° to the rolling direction is performed at quasi-static conditions and room temperature (RT) in order to investigate anisotropy of the material. Small differences were found regarding directions and it was decided to use specimens taken perpendicular to the rolling direction in all subsequent testing.

The tensile tests at high temperature and high strain-rate conditions were performed in an Instron VHS 100/160-20 test machine which has a maximum piston speed of 20 m/s. In Figure 1 the principal features of the specimen geometry are outlined. The straight part of the specimen is 5 mm wide. At one end there is a bolt hole for attachment to the load cell on the test machine and at the other end there is a 300 mm long head so that the grip can slide along the specimen head during acceleration and attach at the upper end when it has reached the desired speed. The straight length and the gauge length are 74 and 50 mm respectively except for the specimens that are used for the highest strain rates for which the corresponding lengths are 44 and 20 mm. This shorter length is necessary in order to reach the highest strain rates because the piston speed is limited to 20 m/s.

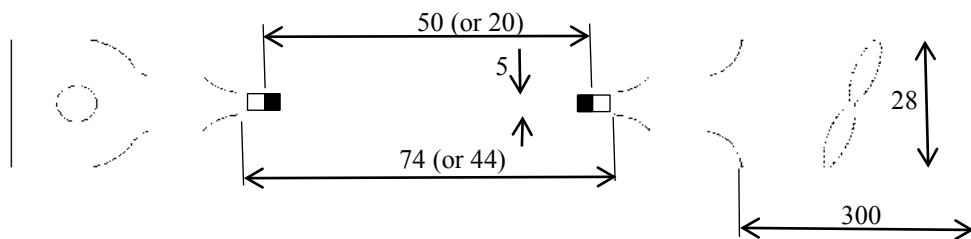


Figure 1. Sketch of specimen geometry.

Elongation of the gauge length during the tensile loading is measured using a dual channel optical system (Zimmer 100D) that monitors the position of the contrast line between a black and a white area. The output is an analogue signal proportional to displacement and elongation is taken as the difference between the two displacements. The optical system has sufficient dynamic properties for measurement of the transient event. For measurement of the

transient force signal a stiff strain gauge based force transducer was designed and built in house. The dynamic response of the force transducer was carefully investigated and it is compensated through a calibration process where a transfer function between the actual force in the specimen and the measured force is used.

High temperatures are obtained through induction heating of the straight part of the specimen. The induction equipment is a SINAC 5 SH from EFD-induction with a coil that has been specially designed and made in-house for the purpose. The temperature is in closed loop control using a thermocouple welded to the centre of the specimen. In order to obtain useful data from the tests, temperature variation must be small over the gauge length of the specimen. This was validated using a thermo-camera. In Figure 2 temperature profiles along the specimen captured with the camera are shown. The profiles are captured at four heating tests on the same specimen with target temperature 585 °C.

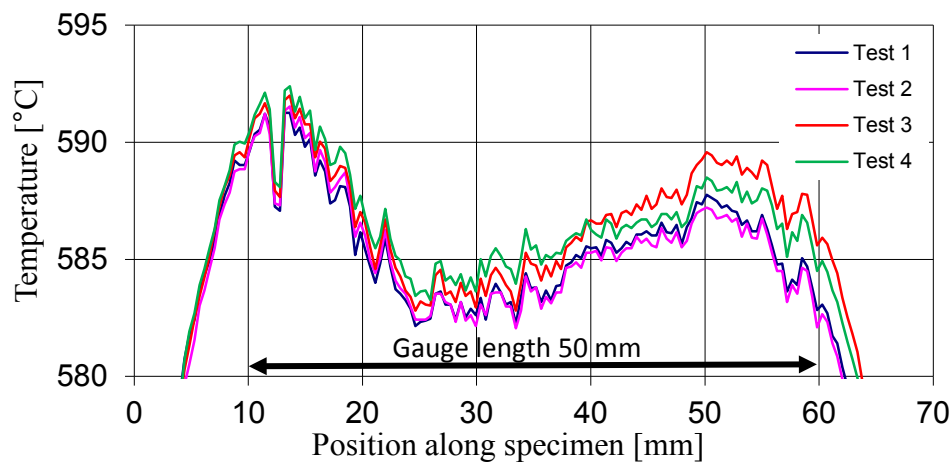


Figure 2. Measured temperature profiles along specimen.

It is believed that the noisy appearance of the curves in Figure 2 is caused by small variations in emission factor since it is almost exactly repeated for all four tests and it is improbable that the temperature varies on such small length scale. The variation with a length scale of about 40 mm is interpreted as a true temperature variation caused by inhomogeneity in the induction field and/or in the cooling by conduction and convection. This temperature variation of about ± 5 °C at 585 °C is considered acceptable. The heating method is thus validated for the 50 mm specimen and a similar validation was also performed for the shorter specimen.

Testing was performed at RT, 550 and 650 °C and at the nominal strain rates 1, 80, 400 and 1000 s⁻¹. Three specimens at each combination were tested. Specimens with gauge length 20 mm were used in the tests with the highest strain rate and in the other tests the gauge length was 50 mm (see Figure 1). The test procedure started with mounting of the specimen to the load cell with a bolt through the hole at its lower end. The upper end is free to slide through the jaws of the spring loaded and locked upper grip which is of wedge-type. Heating

to a pre-set temperature is done in about 10 seconds and after a hold time of about one minute the test is set off. The upper grip accelerates and when it reaches the pre-set velocity the grip lock is released and the jaws attach to the long specimen head. During loading and deformation to fracture which takes about 300 microseconds for the highest strain rate, force and elongation are measured. Sampling of the transient signals is done with a sample rate that gives sufficient resolution of the time signals.

2.3 Evaluation of parameters

In order to fit the material parameters to the data from the tensile testing a least squares approach using MATLAB was developed. Because of the difference in structure for the two models, slightly different approaches were used to find the material parameters. However, common for the two approaches is that the result from each tested specimen is given the same weight in the optimisation. This basic principle eliminates influence from variation in number of digital information points between different experiments.

For the JC-model the initial step was to fit the first parenthesis of eq (1) with the quasi-static tensile tests at RT. First the parameter A is manually evaluated as $R_{p0.2}$ which is the stress at the intersection between the stress strain curve and the side-shifted initial elastic slope of the stress strain curve to 0.2% strain. Then the parameters B and n were fitted to the quasi-static tensile tests at RT, 293K, using the MATLAB subroutine **lsqnonlin**, which solves non-linear least square problems using a trust-region-reflective model. The strain rate of the tensile tests used to evaluate the parameters in the first parenthesis, 0.002 s^{-1} , is set as the reference strain rate $\dot{\epsilon}_{0p}$. In the next step, the quasi-static tests at elevated temperatures are used in order to get a first approximation of the thermal softening parameter m . Next, the temperature increase due to plastic work ΔT was calculated as

$$\Delta T = \frac{\beta}{\rho c_p} \int \sigma(\epsilon_p) d\epsilon_p \quad (3)$$

where β is the Taylor Quinny coefficient, assumed to be 0.9, ρ is the density and c_p is the specific heat coefficient. $\sigma(\epsilon_p)$ is the experimentally obtained stress-strain relation which is numerically integrated. With the change in temperature due to plastic work and the approximate thermal softening parameter known, the yield stress compensated for thermal softening was calculated as

$$\sigma_y^{comp} = \frac{\sigma_y}{1 - \left(\frac{\Delta T}{T_m - T_{test}} \right)^m} \quad (4)$$

where T_m is the melting point of the material, 1573K for alloy 718, and T_{test} is the temperature at which the test was performed. With this thermally compensated yield stress an isothermal parameter C for the strain-rate hardening (see eq (1)) was obtained by least squares fitting to experiments with different strain rates. With the isothermal rate hardening parameter known, a more accurate value of the thermal softening parameter could be calculated using the tests at all strain rates. The process of obtaining the thermal softening and the rate hardening parameters was then repeated until convergence was reached.

In the case of the ZA-model all experimental data were used in a simultaneous fitting process of the seven parameters in eq (2). As for the JC-model the subroutine **lsqnonlin** was used for the optimisation.

2.4 Validation experiment

An instrumented reverse impact experiment was designed to validate the models with evaluated parameters. The principle of the experiment is shown in Figure 3. A circular disc of the tested sheet material with diameter 46 mm and thickness 1.6 mm is accelerated through the barrel of an air gun. The disc is loosely attached to a guide and held in a perpendicular orientation. It impacts the end of a 10 mm steel rod that is parallel with the barrel. The force history has a duration of about 170 microseconds. It is measured with the aid of strain gauges glued to the rod which is long enough to contain the elastic wave generated by the impact force without reflections interfering at the strain gauges. The velocity of the impact is measured with the aid of two laser detectors. A semi spherical tip of tungsten-carbide at the impacted end prevents the rod from being plastically deformed at the impact point. A more detailed description of the experimental set-up is given in [9]. Only experiments at RT are performed in this work.

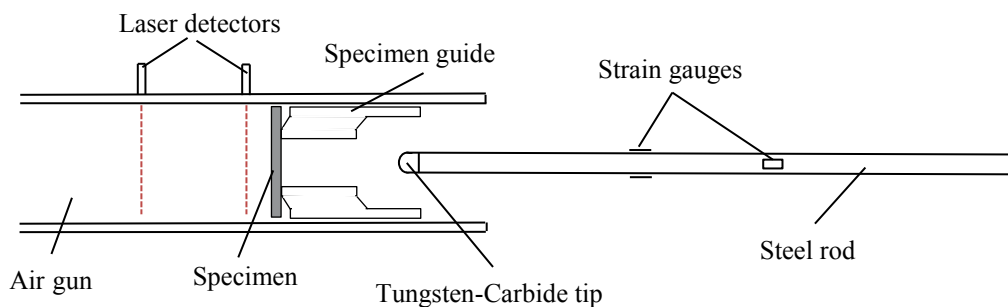


Figure 3. Principal set-up of impact experiment for validation.

The design of the experiment is chosen so that the disc is free from all external influences at the instant of impact and thus friction and/or boundary conditions at fixtures need not be considered. Therefore simulation of the experiment is comparatively simple and straightforward. Simulations are performed with the software LS-DYNA using eight-node brick elements with a smallest size of 0.2 mm. See [9] for more details of the simulation. The output from the experiment is the impact velocity and the force history at the strain gauge position and in the simulations the velocity is used as a primary quantity and the force history is simulated and compared to the experimental result. As the investigation concerns plastic behaviour of the material the impact velocity was held below 50 m/s, which is low enough to avoid visible fracture in the specimens.

3 RESULTS AND DISCUSSION

The primary output from the calibration experiments described in 2.2 is in the form of time histories of axial force on the specimen and elongation of the gauge length. From these data true stress and true strain are evaluated. All combinations of strain rates and temperatures (with repetitions) are comprised in the bulk of experimental results that is the basis for extraction of model parameters. The studied material models are JC and ZA according to eq (1) and (2) in 2.1 above. Evaluation of model parameters is performed as described in 2.3 above. Obtained optimal values of the model parameters are presented in Table 1 for JC and in Table 2 for ZA.

Table 1. Optimal parameters for JC (eq(1))

	A [MPa]	B [MPa]	n [-]	C [-]	m [-]
JC	1176	1456	0.5307	3.54e-3	1.740

Table 2. Optimal parameters for ZA (eq(2))

	σ_a [MPa]	A [MPa]	α_0 [K ⁻¹]	α_1 [K ⁻¹]	B [MPa]	β_0 [K ⁻¹]	β_1 [K ⁻¹]
ZA	837.6	1136	-3.24e-4	-1.27e-4	1033	3.61e-3	2.27e-3

In the determination of model parameters an initial guess of the parameter set is given as a starting vector for the optimisation procedure. For the JC-model the initial guess was one of the parameter sets for alloy 718 found in the literature [5]. For the ZA-model no suggested parameter set was found in literature for alloy 718. Instead, parameters for nickel alloy 690 [10] were used as initial guess. In order to make sure that the obtained optimal values of the parameters do not represent a local minimum dependent on the initial guess, a robustness analysis was performed where the initial guess of parameter was varied over a large interval. As the results did not change when the initial guess was changed the obtained optimal parameter sets were considered as robust best fits of the models to the experimental data.

In Figure 4 and 5 the models with parameters according to Table 1 and Table 2 are plotted (dashed lines) for the same strain rates and temperatures as in the calibration experiments. The results from the experiments are also shown in the diagrams (solid lines) for comparison. The results at RT are plotted in blue colour while the results at 550°C and 650°C are plotted in green and red respectively. Both models seem to agree reasonably with the experiments. The JC model agrees better at low strains than the ZA model while the ZA model more accurately captures the effects of the thermal softening.

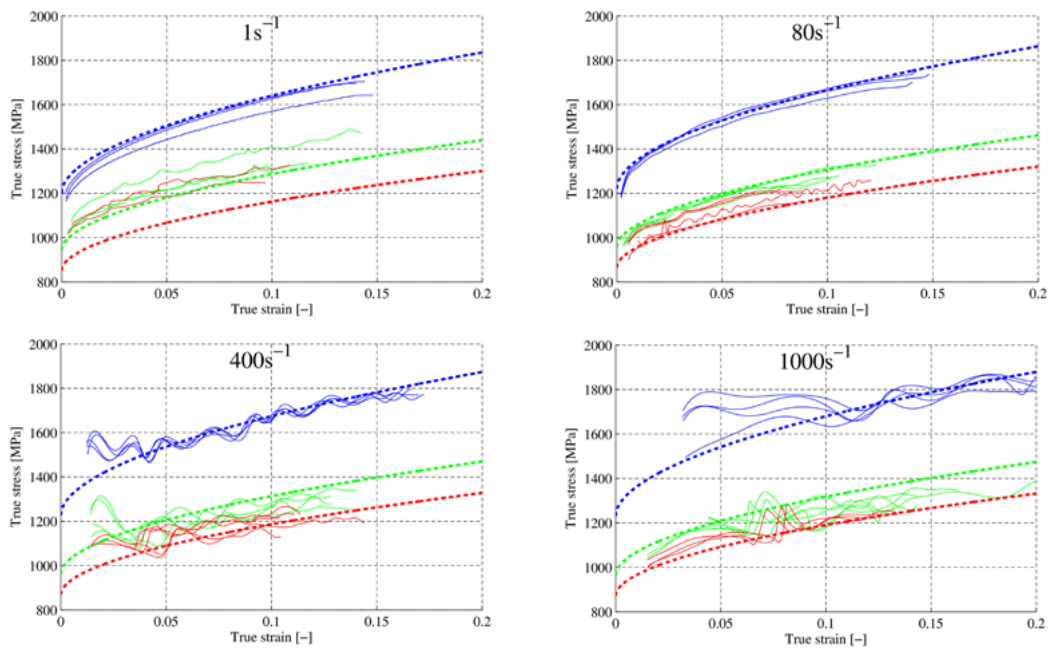


Figure 4. Experimental results (solid) and fitted Johnson-Cook model (dashed). RT -, 550°C - and 650°C -.

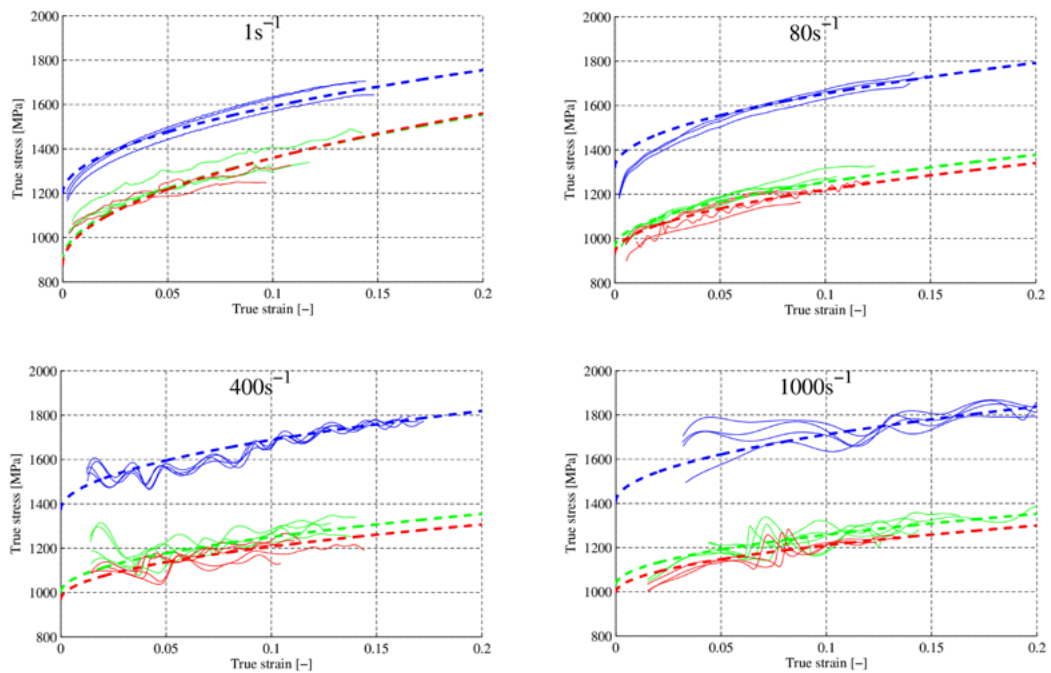


Figure 5. Experimental results (solid) and fitted Zerilli-Armstrong model (dashed). RT -, 550°C - and 650°C -.

The experimental stress-strain data shown in Figure 4 and 5, which the optimisation is based on, are truncated at the beginning. The reason is that dynamic effects from the mechanical equipment as well as elastic strains in the tested material are disturbances that do not represent plasticity in the material. It is observed from Figure 4 and 5 that dynamic disturbances still remain at higher strain rates. A more radical truncation would have some effect on the optimal parameter sets but it is believed that the effect would only be small. It must also be remembered that the experimental strain rates are nominal values based on piston speed and specimen geometry. Due to dynamics in the experiment the strain rate will vary to some extent during the experiment and one can argue that the mean value should be calculated and used in the modelling. However, this is not further investigated and quantified here since the material is fairly insensitive to strain rate which makes the effect of the variation less important. It should also be noted that in the procedure for determination of parameters it is presumed that stress and strain are homogeneously distributed over the gauge length of the specimen. This implies that necking must not occur during the tensile test. Using the JC model with obtained parameters, the Considère criterion for necking ($\partial\sigma/\partial\varepsilon=\sigma$) was checked for all rates and temperatures and the result indicates that almost all the data from the tensile tests are gathered before necking occurs. This is also confirmed by the fact that necking is not observed from the specimens after testing.

From the validation experiments described in 2.4 measured force histories as shown in Figure 6 are obtained. Such results obtained at plastic conditions in an impact event are suitable for validation of plastic material models. A useful model must be able to accurately predict the measured force history. Material parameters according to Table 1 and 2 are used in the simulations and in Figure 6 the corresponding results are shown. The simulations were performed in the commercial FE-code LS-DYNA.

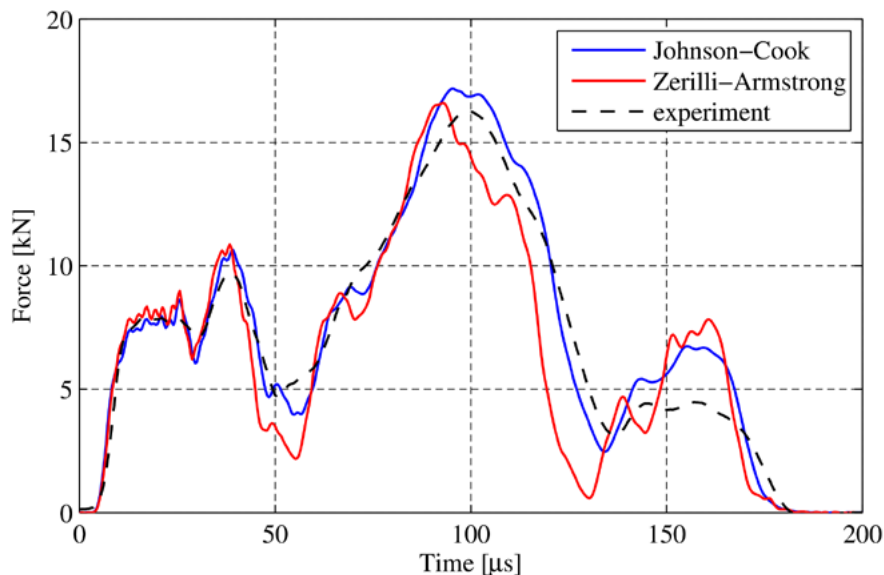


Figure 6. Experimental and simulated impact force histories.

The results seen in Figure 6 show generally good agreement between the experiment and the two material models used. In order to quantify which of the two models that best fits the experiments Van Hove's R-factor method was utilised. The R-factor was computed for each simulation combined with three experimental curves. A comparison factor was then computed as the average of the obtained R-factor values. The value was 1.18 for the JC model and 2.73 for the ZA model. This means that the JC model is better at capturing the behaviour of Alloy 718 at an impact event at RT such as described in section 2.4.

Development of an impact experiment with hot specimens will facilitate validation of models also at high temperatures. Finally it is noted that although one particular material and two models are investigated here, the used methods are general and other materials and models may be studied.

4 CONCLUSIONS

- A method is presented for investigation of material models for plastic deformation under high strain rate and high temperature conditions. The method is used for the investigation of Alloy 718.
- The method includes basic calibration experiments in a high speed testing machine, extraction of model parameters through an optimisation procedure and validation of the result in a specially designed impact experiment.
- The model suggested by Johnson-Cook shows better agreement with the impact experiment than the model suggested by Zerilli-Armstrong does for the tested material at room temperature.

ACKNOWLEDGEMENTS

Economic support for this work is supplied by VINNOVA through the project NFFP5 nr 2009-01242 which is gratefully acknowledged. The authors want to thank Mr Johan Forsman and Mr Dennis Jacobsson at GKN Aerospace for good cooperation and advice. Also the help with some experimental issues by Mr Jan Granström and Mr David Enqvist is acknowledged.

REFERENCES

- [1] Avril, S. et al. Overview of identification methods of mechanical parameters based on full-field measurements. *Experimental Mechanics* 48 (2008) 381–402
- [2] Kajberg, J. Sundin, K.G. Material characterisation using high-temperature Split Hopkinson pressure bar. *Journal of Materials Processing Technology* (2012)
- [3] DeMange, J.J. et al. Effects of material microstructure on blunt projectile penetration of a nickel-based super alloy. *Int. J. of Impact Engng.* 36 (8) (2009) 1027-1043.
- [4] Kobayashi, T. et al. Plastic flow behavior of Inconel 718 under dynamic shear loads. *Int. J. of Impact Engng* 35 (5) (2008) 389-396.
- [5] Pereira, J.M. and Lerch, B.A. Effects of heat treatment on the ballistic impact properties of Inconel 718 for jet engine fan containment applications. *Int. J. of Impact Engng* 25 (8) (2001) 715-733.
- [6] Zhou, Z. et al. A finite element study of thermal relaxation of residual stress in laser shock peened IN718 superalloy. *Int. J. of Impact Engng* 38 (7) (2011) 590-596.
- [7] Johnson, G.R. and Cook, W.H. A constitutive model and data for metals subjected to large strains, high strain rates and high temperatures. *Proceedings of the 7th Int. Symposium on Ballistics* 21 (1983) 541-547.
- [8] Zerilli, F.J. Dislocation mechanics-based constitutive equations. *Metallurgical and Materials Transactions A.* 35 (9) (2004) 2547-2555.
- [9] Sjöberg, T. et al. Comparative investigation of parameters in the Johnson-Cook model for Alloy 718 through instrumented reverse impact experiments. (*Submitted for publication*)
- [10] Lee, W. and Sun, T. Plastic flow behaviour of Inconel 690 super alloy under compressive impact loading. *Materials transactions* 45 (7) (2004) 2339-2345.